FUNCTIONAL SUBSTRATES FOR FLEXIBLE ORGANIC PHOTOVOLTAIC CELLS

M. Niggemann[a,b], D. Ruf[a], B. Bläsi[a], M. Glatthaar[b], M. Riede[a], C. Müller[c], B. Zimmermann[b] and A. Gombert[a]

[a] Fraunhofer Institute for Solar Energy Systems (ISE), Heidenhofstr. 2, 79110 Freiburg, Germany;
[b] Material Research Center Freiburg (FMF), Stefan-Meier-Str. 21, 79104 Freiburg, Germany;
[c] Institute of Microsystem Technology (IMTEK), Georges-Köhler-Allee 103, 79110 Freiburg, Germany

ABSTRACT

Along with efficiency and lifetime, costs are one of the most important aspects for the commercialization of organic solar cells. Thinking of large scale production of organic solar cells by an efficient reel-to-reel process, the materials are expected to determine the costs of the final product. Our approach is to develop functional substrates for organic solar cells which have the potential for cost effective production. The functionality is obtained by combining periodically microstructured substrates with lamellar electrode structures. Such structured substrates were fabricated by cost effective replication from masterstructures that were generated by large area interference lithography. Two cell architectures were investigated - holographic microprisms and interdigital buried nanoelectrodes. A structure period of $20\mu m$ in combination with a $2\mu m$ wide metal grid was chosen for the microprism cells based on the results of electrical calculations. Current-voltage curves with reasonable fill factors were measured for these devices. A significant light trapping effect was predicted from optical simulations. Interdigital buried nanoelectrodes are embedded in the photoactive layer of the solar cell. Separated interdigital metal electrodes with a sufficiently high parallel resistance were manufactured despite a small electrode distance below 400 nm. Experimental results on first photovoltaic devices will be presented. We observe an insufficient rectification of the photovoltaic device which we attribute to partial electron injection into the gold anode.

Keywords: light trapping, microstructure, nanoelectrode, organic solar cell, interference lithography

1. INTRODUCTION

Using organic semiconducting materials in solar cells is a new approach with promising possibilities. The great potential of low cost production combined with mechanical flexibility gives rise to new applications. Due to the relatively simple fabrication process from solution and the mechanical flexibility, the production of organic solar cells by the cost effective reel-to-reel process appears promising. Along with efficiency and lifetime, the costs are one of the most important aspects for commercialization of organic solar cells. The most widely used transparent electrode material for organic solar cells is indium tin oxide (ITO). It is expected that ITO will be a major cost factor for organic solar cells *. A promising concept of an organic solar cell is the so called bulk heterojunction solar cell.[2] The most common donor- and acceptor components are poly-3(hexyl-thiophene)(P3HT) and [6,6]-phenyl C61 - butyric acid methyl ester (PCBM, a C_{60}-derivative) respectively.[3] Standard devices are built up on ITO coated on glass or on polymer serving as a transparent electrode. Subsequently the organic layers, poly(3,4-ethylene-dioxy-thiophene)-poly(styrene sulfonate) (PEDOT-PSS), serving as anode and the photoactive blend are deposited from solution. Finally, the aluminium electrode is evaporated on top. The efficiency is still limited by the small charge carrier mobilities and the insufficient overlap between the solar spectrum and the absorption of the organic photoactive components. Efficiencies up to 4% are reported for this type of an organic solar cell. Motivated by the demands for efficient and cost effective organic solar cells, we develop cell architectures

Further author information: E-mail: Michael.Niggemann@ise.fraunhofer.de, Telephone: +049 (0)761 2034798

*Due to the large consumption by the flat panel technologies, the indium price rose from 70 $US\$/kg$ (06/2002) up to 970 $US\$/kg$ (06/2005) in the last three years and further growth in consumption is expected in the future.[1]

Organic Photovoltaics VI, edited by Zakya H. Kafafi, Paul A. Lane,
Proc. of SPIE Vol. 5938, 593802, (2005) · 0277-786X/05/$15 · doi: 10.1117/12.617196

based on microstrucured substrates. The three dimensional surface of the substrate allows to design electrode structures and geometries which contribute to an efficient charge collection and light absorption.

Interference lithography offers the possibility to generate periodic surface relief structures in a large variety of shapes and dimensions from subwavelengths nanostructures (200 nm grating period) up to several tens of micrometres on large areas up to $1m^2$. The interference pattern is recorded by a thin photoresist layer. In a subsequent developing process, the intensity profile of the interference pattern is transferred into a three-dimensional surface relief. The photoresist structures can be replicated into nickel stamps for subsequent microreplication into a suitable substrate material. Roller UV embossing of microstructures is a technology which is already established as an industrial process (e.g. Autotype Ltd, Wantage England). This method allows very good reproducibility and very high resolution and is well suited for mass production as the set-up is realised in a reel-to-reel process. Both types of substrates - nanolelectrodes and microprisms - which will be presented in the following, were produced by these processes.

2. MICROPRISM SUBSTRATE

2.1. Introduction

We report on a cell architecture for organic solar cells based on a holographic microprism substrate. In principle, the geometry can be described by a folded planar solar cell (figure 1). This set-up comprises two advantages in comparison to the standard organic solar cell. First, the ITO-electrode is substituted by a highly conductive polymer layer (PEDOT:PSS formulation PEDOT CPP 105 D by H.C. Starck) with a supporting metal grid located in the valley of the structure. Second, the microprism structure contributes to an increased light absorption due to a twofold reflection of the incident light. Extensive investigations have been carried out on micromachined prismatic structures and were presented elsewhere.[4] The relevant results from optical and electrical simulations will be summarized here. Solar cells based on micromachined prismatic structures suffered from electrical shunt defects predominately at the sharp tips of the structures. Holographic microprisms have round tips which allow a better wetting of the photoactive layer in this region. As a consequence the probability for electrical shunts is reduced.

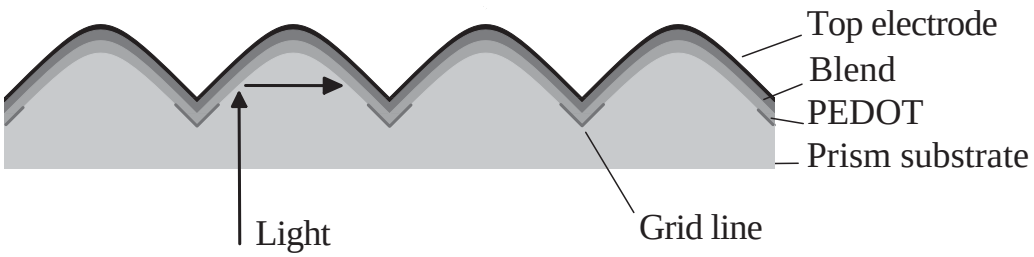

Figure 1. Cross section of an organic microprism solar cell.

2.2. Optical Simulations

The calculations of the absorptance in distinct layers of the solar cell were performed by Rigorous Coupled Wave Analysis (RCWA), a method which was implemented for describing near-field phenomena at corrugated interfaces.[5–8] Investigations on diffraction gratings for light trapping in organic solar cells based on RCWA calculations are presented elsewhere.[9] Optical constants are taken for the MDMO-PPV/PCBM system[10] which is comparable to the P3HT/PCBM system with a slight shift in the complex refractive index towards shorter wavelengths. Optical constants for the PEDOT layer were determined for the formulation AI4083 purchased from Bayer and may deviate slightly from the optical constants of the highly conductive PEDOT CPP 105 D which was used in these devices.[10] The thickness of the photoactive layer and the PEDOT layer was 100 nm. Both polarisations of the incident light - transversal electric (TE) and transversal magnetic (TM) were considered.

The optics of the thin film system which is deposited on the prismatic structure is investigated by simulating the effect of inclined incident light onto the thin film system and by considering a second absorption process. As a consequence, the influence of the rounded tip of the structure on the light absorption will not be considered here. The light is incident from a semi-infinite non absorbing medium with a refractive index of 1.5. The incident angle is varied from 0° (normal incidence) to 80°. In a first approximation the short-circuit current density is calculated from the spectral absorption in the blend layer and the solar spectrum. An internal quantum efficiency of unity is assumed.[3] Calculations for polarised and unpolarised light are shown in figure 2 (left).

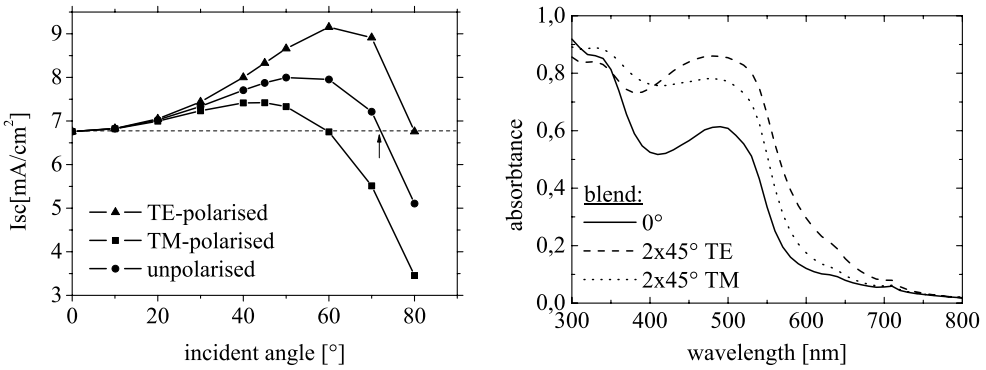

Figure 2. Left: Calculated angle dependent photocurrent for TE- and TM-polarisation according to an assumed internal quantum efficiency of unity. Right: Spectral absorptance of the photoactive layer (right) for a twofold reflection under 45° in TE- and TM-polarisation in comparison to the case of normal incidence on a planar thin film system (100 *nm* PEDOT, 100 *nm* MDMO-PPV/PCBM-blend, 100 *nm* aluminium).

When the incident angle is increased from normal incidence (0°) up to 80°, the calculated short-circuit current for TE- and TM-polarisation increases up to a certain peak value. For TE-polarisation, the short-circuit current increases and reaches a maximum of 35.5% at an angle of 60°, whereas for TM-polarisation a maxiumum increase of 9.8% is calculated at an angle of 45°. For unpolarised light, the peak position can be found at 50° leading to an increase of 18.3%. The reason for an increased charge carrier generation with increasing incident angle can be found in an increase of the spectral absorptance at larger wavelengths in the photoactive layer (not shown here). The overall photocurrent is increased because of the larger photonflux of the solar spectrum at longer wavelengths. From these initial calculations it can be concluded that inclined incident light on the thin film system should result in an increased short-circuit current in an angular range from 0° to 72° for unpolarised light (see figure 2 (left) intersection with dashed line).

The case of normal incident light on the microprism-structure is investigated here. The light is reflected and partially absorbed twice under an angle of 45°. Of special interest for the solar cell is the absorption in the photoactive layer (see figure 2 (right)). A slightly higher absorptance in the photo-active layer can be observed for TE-polarisation over the spectral range from 400 *nm* to 800 *nm*. From convolution of the spectral absorption in the photoactive layer with the AM1.5 solar spectrum, an increase in absorptance of 55% in TE-polarisation and of 33% in TM-polarisation was calculated relative to the case of normal incident light on a planar solar cell. This leads to an average increase of 44% for unpolarised light. Optical losses due to shadowing by the microgrid are not taken into account here, but will be considered in the following chapter.

2.2.1. Dimensioning of the Microstructure

The dimensions of the microstructure strongly affect the efficiency of the solar cell. This becomes obvious as the period of the microprism structure defines the distance of the grid lines. Ohmic losses have to be minimized by a sufficiently small grid distance, whereas the ratio between the lattice distance of the grid and the width of the conducting lines should be as large as possible in order to minimize the shadowing effect. In addition, the metal grid lines have to be sufficiently conductive so that the series resistance is minimized. The contribution

of the aluminium top electrode and of the gold grid to the series resistance are neglected. The current-voltage characteristics of an infinitesimal small elementary cell with $V_{oc} = 600\ mV$, $I_{sc} = 15\ mA/cm^2$ and $FF = 0.55$ were taken as input parameters for the calculations. Such an elementary cell would have an efficiency of 5%. In order to determine the optimum lattice distance for a given type of structure, calculations were made for different gridline widths ranging from 2 μm up to 40 μm and for a sheet resistance varying between 10^4 $\Omega/\square$ and 10^7 $\Omega/\square$ (figure 3).

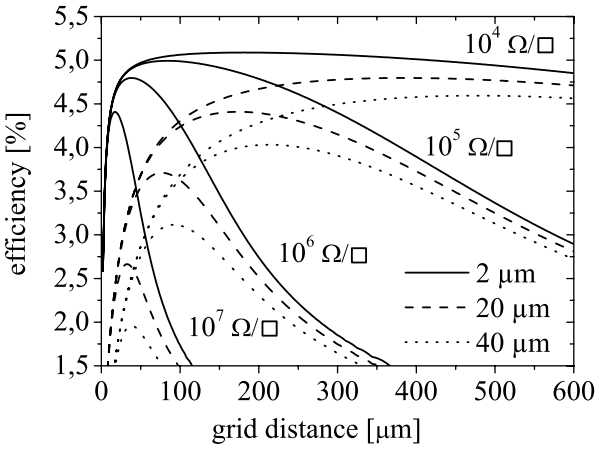

Figure 3. Calculation of the efficiency depending on the grid distance for different sheet resistances of the PEDOT layer and various widths of the gridlines.

The two competing loss mechanisms - ohmic losses and losses by shadowing - determine the characteristics of the calculations. The steepness of the rising efficiency with increasing grid distance is strongly affected by the shadowing losses caused by the grid lines, whereas the decaying efficiency at larger grid distances is determined by the PEDOT CPP 105 D sheet resistance and therefore by the ohmic losses. The geometry of the microprism structure is considered in the calculations by an effectively reduced current density caused by the tilted absorbing surface. It is intuitive that the efficiency of the cell is weakly affected by the grid distance for small widths of gridlines and a small sheet resistance of the PEDOT. To minimise absorption losses in the PEDOT layer, the thickness should range between 80 nm and 120 nm. A strong variation of the PEDOT sheet resistance between approximately 10^4 $\Omega/\square$ and 10^5 $\Omega/\square$ was measured for film thickness in this range. Assuming a conservative value of 10^5 $\Omega/\square$ and a realistic width of the gold grid of 2 μm for structures generated by interference lithography, an optimum grid distance of 22 μm $-$ 215 μm ($\leq 5\%$ deviation from peak efficiency) can be extracted from the calculations shown in figure 3. This value corresponds to a period of the microprism structure of 16 μm $-$ 152 μm (The grid distance is calculated from the pathlengths on the prismatic surface).

2.3. Experimental

Preliminary experiments were carried out on micromachined prismstructures with a period of 100 μm and fairly sharp tips. The insufficient wetting of the photoactive layer on these tips was the origin of electrical shunts and therefore resulted in small fill factors of the photovoltaic cells. The holographic microprism structures with a period of 20 μm and rounded tips were generated by interference lithography and subsequent microreplication. The metal grid was made by a combination of evaporation processes under inclined incident angles using the microstructure as a self aligning shadow mask. 50 nm thick and $2-3$ μm wide gold grid lines were obtained. A chrome layer (8 mn thick) which was evaporated before guarantees a good adhesion. The effective sheet resistance of the grid was $\approx$ 10 $\Omega/\square$ which is comparable to the sheet resistance of commercially available ITO. The polymer anode (PEDOT CPP105D) was spin coated at 1000 rpm for 60 s. The thickness of the PEDOT layer was investigated by scanning electron microscopy (SEM). In contrast to previously investigated

micromachined prismatic structures with sharp tips, a homogenous coating of the rounded tips with a film thickness of approximately 100 nm was observed (see figure 4). However, film thickness exceeding 400 nm can be observed in the valley of the structure. An improvement of the homogeneity is expected by further optimizing the viscosity and spin coating parameters.

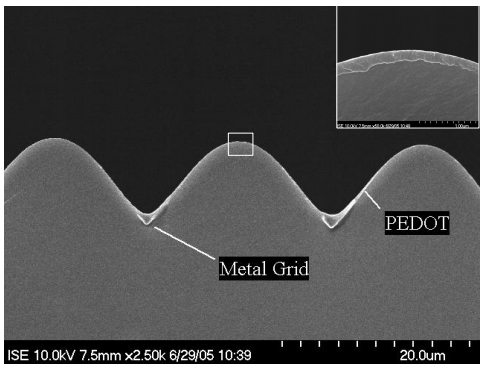

Figure 4. Cross section of a holographic microprism substrate carrying a microgrid and coated with the polymer anode (Scanning electron microscopy image).

Preliminary investigations were made with a blend solution of 15 mg PCBM and 10 mg P3HT dissolved in 1 ml tetrahydronaphtalene. In contrast to the solvent chlorobenzene, post treatment is not required in this case.[11] The photoactive layer was spincoated at 500 rpm for 60 s. Although the thickness of the blend layer could not be measured precisely because of preparation artefacts, we expect from visible inspection a thickness significantly smaller than the film thickness on planar reference samples. The spin coating parameters and the viscosity of the blend solution have not been optimized yet.

A current-voltage characteristics of a sample is shown in figure 5. The efficiency of 0,84% is low in comparison to planar reference cells ($\eta = 1.5\%$). The major limitation is the low short circuit current which we attribute to the thin absorber. The open circuit voltage of 475 mV is within the fluctuations of the open circuit voltages of planar reference devices based on ITO subtrates. Nevertheless, it is lower than the often reported 550 mV for planar ITO based solar cells spin coated from a chlorobenzene solution. The reasonable fill factor of 0.52 and the differential resistances Rs=(3.8 Ωcm^2) at 1.0 V and Rp=840 Ωcm^2 (under illumination) at 0 V were extracted from the current-voltage characteristics. These values are comparable to characteristic data from planar reference cells.

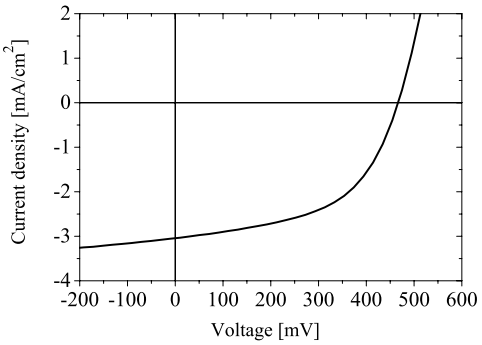

Figure 5. Current-voltage characteristics of microprism solar cell (V_{oc} = 475 mV, I_{sc} = 3.0 mA/cm^2, FF = 0.52 $\eta = 0.84\%$ (885 mW/cm^2).

We conclude that the holographic microprisms solar cell architecture allows an efficient collection of the

charge carriers. The effect of creating electrical shunts even for thin absorbing films at the tips of the structure is not observed to be critical. In order to prove the light trapping effect which was predicted from simulation calculations, the coating of the photoactive layer has to be optimized. A homogeneous and sufficiently thick absorber has to be achieved.

3. INTERDIGITAL NANOELECTRODES

3.1. Introduction

Buried nanoelectrodes are vertically orientated electrodes embedded in the photoactive layer of the solar cell. The substitution of both planar electrodes by buried nanoelectrodes results in an interdigital electrode set-up (figure 6).

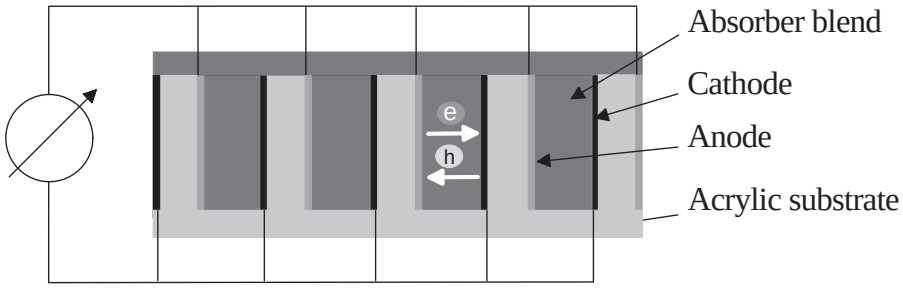

Figure 6. Concept of interdigital buried nanoelectrodes.

In contrast to the concept of the microprism solar cell presented in section 2, the dimensions of the buried nanoelectrodes are comparable to the thickness of the organic films. The period of the microstructure ($\Lambda = 720\ nm$) is in the range of the wavelength of the incident light. In principle, this architecture follows the requirement of separating the light absorption from the charge carrier transport. Hence, the effective thickness of the absorber can be increased while keeping the distance of the electrodes small enough for an efficient charge extraction. However, technological limitations with respect to the aspect ratio of the structures have to be considered. In contrast to the planar solar cell architecture based on an ITO substrate, both electrodes are deposited prior to the application of the photoactive film. This can be of advantage for the device preparation because no vacuum deposition step is required after the deposition of the organic compounds. Another feature is the absence of a highly reflecting back electrode. This makes semitransparent applications possible. The interface formation is an important issue. Suitable contacts with high selectivity are under investigation. As the dimensions of these structures are in the range of the wavelength of light, near-field optics plays an important role. Strong interactions of the light in terms of high absorption in TM-polarisation are observed in preliminary simulations.

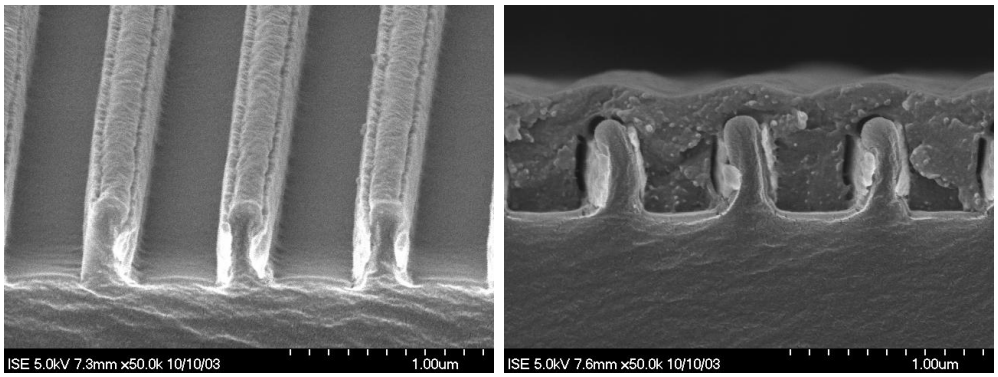

Figure 7. Left: Nano-structured substrate with separated interdigital nanoelectrodes. Right: Nanoelectrode structure filled with the photoactive material.

3.2. Experimental

The substrate for buried nanoelectrodes is made by replication of holographically created structures into an acrylic UV curable photopolymer. The dimensions of the microstructure are a lamellae period of 720 nm, a depth of approximately 400 nm and a cavity width of 400 nm. Two electrodes can be realised by oblique evaporation of different metals (see figure 7 (left)). Additional process steps are required in order to obtain seperated interdigital electrodes. The areas of the respective electrodes are defined by shadow masks during evaporation under inclined angles, whereas the interconnection of the grid lines is made by evaporation of a stripe perpendicular to the lamellae from normal incidence. The electrode materials have to provide good contacts for the organic semiconductor. One prerequisite is the matching of the electrode workfunction to the respective quasi Fermi potentials of the semiconductor. Investigations on inverting the layer sequence in organic solar cells have shown, that titanium is suited as a predeposited cathode.[12] The conductivity of the titanium electrode was enhanced by an underlying aluminium layer. The anode was made from gold which is known to serve as a hole contact for field effect measurements on P3HT.

The interdigital electrode array was investigated by impedance spectroscopy. It is expected that the lamellar orientated electrodes show a capacitive behaviour. This behaviour is described as two parallel capacitors, distinguished in their dielectric materials. One is formed by the electrodes opposing the acrylic substrate lamellae and the other by the same electrodes opposing the cavities. Impedance measurements were carried out in order to determine the capacitance and the shunt resistance of the interdigital electrode array. A capacitance of 30 pF was measured which proves the existence of an interdigital electrode array which is connected to the bus bars. The shunt resistance strongly affects the efficiency of the photovoltaic device. A parallel resistance of $10^3\ \Omega cm^2$ is sufficiently high.[13] Such values are within reach by providing sufficiently clean preparation conditions. The best result was a shunt resistance of $2.9 \cdot 10^5\ \Omega cm^2$.

After the electrical characterization of the nanoelectrode substrate, the cavities were filled by applying the solution of the photoactive blend. The current voltage characteristics of two samples with a low shunt resistance of 38 Ωcm^2 and a high shunt resistance of $2.9 \cdot 10^5\ \Omega cm^2$ (determined prior to the deposition of the photoactive polymer) are shown in figure 8 (left). The performance of the low shunt resistance cell is significantly lower as expected. Nevertheless, the small fill factor of 25% of the high shunt resistance photovoltaic cell can only be explained by the electric contacts rather than by a low shunt resistance due to direct contact of the eletrodes. This becomes obvious in figure 8 (right). The rectification of the device is rather low. We attribute this effect on an insuffiecient selectivity of the gold electrode for the repective charge carriers. Both types of charge carriers can be injected into the gold electrode. This is confirmed by investigations on planar solar cells using gold as electrons collecting material.[14] A detailed investigation on interface dipole layers between C_{60} and Au is presented by Veenstra et al..[15] A shift of the LUMO of the C_{60} derivative to the Fermi level of the metal electrode was observed.

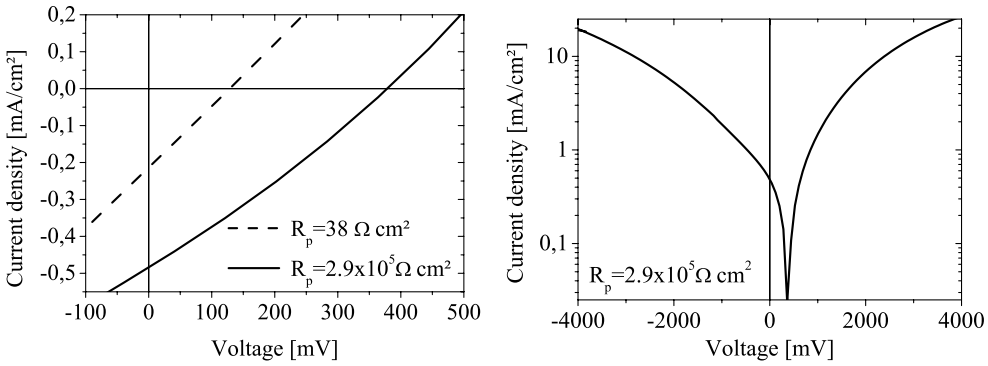

Figure 8. Left: Current-voltage characteristics of two photovoltaic devices based on interdigital nanoelectrodes with different parallel resistances. Right: Logarithmic current-voltage characteristic of the sample with the highest parallel resistance $R_p = 2.9 \cdot 10^5\ \Omega cm^2$ ($FF = 25\%$, $I_{SC} = 0.5\ mA/cm^2$, $U_{OC} = 380\ mV$, $Pin = 100\ mW/cm^2$, $\eta = 0.05\%$)

Interdigital nanoelectrodes can be realized on small areas (5 mm^2) with sufficiently large parallel resistance. The proof of principle has been demonstrated. Nevertheless, the hole contact needs to be optimized in order to allow an efficient charge collection. An improvement is expected by either coating the anode by electropolymerisation of PEDOT[16] or by another electrode material like a thin intermediate layer of palladium.[17]

4. OUTLOOK

Using nano- and microstructured substrates for organic electronic devices widens the possibilities to optimize or even to create novel devices. We demonstrated the suitability of holographic microprisms for organic photovoltaic devices. More accurate optical modelling has to take into account the inhomogeneous thickness of the thin films and the rounded tip. The coating of the thin films on the corrugated surfaces needs to be optimized. Therefore it is necessary to tailor the rheological properties of the solutions. In order to maintain a cost effective substrate, the deposition of the microgrid by thermal evaporation processes has to be substituted by a deposition process from solution or paste. Finally, upscaling will be an important issue in the future. Fortunately the technology for large area microstructured substrates is already available.

Interdigital buried nanoelectrodes are still at an early stage of the investigations. The development of suitable electrodes will be a future topic. The potential of this device architecture for photovoltaic applications has to be further investigated by optical modelling and experiments. Besides the application for solar cells, the concept of vertical interdigital nanoelectrodes with distances down to 200 nm offers a wide range of different applications like sensors, organic field effect transistors (OFET) and organic light emitting devices (OLED).

ACKNOWLEDGMENTS

Special thanks to Autotype Ltd, Wantage England for the replication of the microstructures.

REFERENCES

1. Metals Place. Producer sees no slide in indium prices. 2005.
2. S. E. Shaheen, C. J. Brabec, N. S. Sariciftci, F. Padinger, T. Fromherz, and J. C. Hummelen. 2.5% efficient organic plastic solar cells. *Applied Physics Letters*, 78(6):841–843, 2001.
3. P. Schilinsky, C. Waldauf, and C. J. Brabec. Recombination and loss analysis in polythiophene based bulk heterojunction photodetectors. *Applied Physics Letters*, 81(20):3885–3887, 2002.
4. M. Niggemann, M. Glatthaar, A. Gombert, P. Lewer, C. Mueller, and J. Wagner. Functional microprism substrate for organic solar cells. *Thin Solid Films*, submitted, 2005.

5. M. G. Moharam and T. K. Gaylord. Diffraction analysis of dielectric surface-relief gratings. *Journal of the Optical Society of America*, 72(10):1385–1392, 1982.
6. M. G. Moharam and T. K. Gaylord. Rigorous coupled wave analysis of planar diffraction gratings. *Journal of the Optical Society of America A-Optics Image Science and Vision*, 71:811–818, 1981.
7. P. Lalanne and G. M. Morris. Highly improved convergence of the coupled-wave method for tranversal magnetic polarization. *Journal of the Optical Society of America A-Optics Image Science and Vision*, 13(4):779–784, 1996.
8. P. Lalanne and M. P. Jurek. Computation of the near-field pattern with the coupled-wave method for transverse magnetic polarization. *Journal of Modern Optics*, 45(7):1357–1374, 1998.
9. M. Niggemann, M. Glatthaar, A. Gombert, A. Hinsch, and V. Wittwer. Diffraction gratings and buried nano-electrodes - architectures for organic solar cells. *Thin Solid Films*, 451-452:619–623, 2004.
10. H. Hoppe, N. S. Sariciftci, and D. Meissner. Optical constants of conjugated polymer/fullerene based bulk-heterojunction organic solar cells. *Molecular Crystals and Liquid Crystals*, 385:233–239, 2002.
11. P.Vanlaeke, G.Vanhoyland, J.Poortmans, P.Heremans, J.Manca, C.Deibel, T.Aernouts, and D.Cheyns. Polythiophene based bulk heterojunction solar cells: Morphology and its implications. *Thin Solid Films*, submitted, 2005.
12. M. Glatthaar, M. Niggemann, B. Zimmermann, P Lewer, M. Riede, A Hinsch, and J. Luther. Organic solar cells using inverted layer sequence. *Thin Solid Films*, article in press, 2005.
13. P. Schilinsky, C. Waldauf, J. Hauch, and C. J. Brabec. Simulation of light intensity dependent current characteristics of polymer solar cells. *Journal of Applied Physics*, 95(5):2816–2819, 2004.
14. B.Zimmermann, M.Glatthaar, M.Niggemann, M.Riede, and A.Hinsch. Electroabsorption studies of organic bulk-heterojunction solar cells. *Thin Solid Films*, article in press, 2005.
15. S. C. Veenstra, A. Heeres, G. Hadziioannou, G. A. Sawatzky, and H. T. Jonkman. On interface dipole layers between c-60 and ag or au. *Applied Physics A-Materials Science Processing*, 75(6):661–666, 2002.
16. Xinyan Cui and David C. Martin. Electrochemical deposition and characterization of poly(3,4-ethylenedioxythiophene) on neural microelectrode arrays. *Sensors and Actuators B: Chemical*, 89(1-2):92–102, 2003.
17. V. D. Mihailetchi, L. J. A. Koster, P. W. M. Blom, C. Melzer, B. de Bor, J. K. J. van Duren, and R. A. J. Janssen. Compositional dependence of the performance of mdmo-ppv:pcbm solar cells. 2005.